JAERI-Tech
2001-022

DEVELOPMENT OF THE CENTRIFUGAL PELLET INJECTOR FOR JT-60U

March 2001

Kaname KIZU, Hajime HIRATSUKA, Hisashi ICHIGE, Takaaki IWAHASHI,
Tadayuki SASAJIMA, Kei MASAKI, Noboru SASAKI, Masao HONDA,
Naoyuki MIYA and Nobuyuki HOSOGANE

日本原子力研究所
Japan Atomic Energy Research Institute

本レポートは、日本原子力研究所が不定期に公刊している研究報告書です。
入手の問合わせは、日本原子力研究所研究情報部研究情報課（〒319-1195　茨城県那珂郡東海村）あて、お申し越し下さい。なお、このほかに財団法人原子力弘済会資料センター（〒319-1195　茨城県那珂郡東海村日本原子力研究所内）で複写による実費頒布を行っております。

This report is issued irregularly.
Inquiries about availability of the reports should be addressed to Research Information Division, Department of Intellectual Resources, Japan Atomic Energy Research Institute, Tokai-mura, Naka-gun, Ibaraki-ken 〒319-1195, Japan.

編集兼発行　日本原子力研究所

JAERI－Tech 2001－022

Development of The Centrifugal Pellet Injector for JT-60U

Kaname KIZU, Hajime HIRATSUKA, Hisashi ICHIGE, Takaaki IWAHASHI, Tadayuki SASAJIMA, Kei MASAKI, Noboru SASAKI, Masao HONDA, Naoyuki MIYA and Nobuyuki HOSOGANE

Department of Fusion Facilities
Naka Fusion Research Establishment
Japan Atomic Energy Research Institute
Naka-machi, Naka-gun, Ibaraki-ken

(Received February 8, 2001)

For core fueling of JT-60U plasmas, a repetitive pellet injector which centrifugally accelerates D_2 cubic pellets using a straight rod has been developed. This centrifugal pellet injector can eject trains of up to 40 cubic pellets at frequencies of 1-10 Hz and velocities of 0.3-1.0 km/s. The average pellet mass is 3.6×10^{20} atoms/pellet below 0.7 m/s.

Key techniques for the development were a mesh structured acceleration component for removing gas sublimated from the pellet and a funnel with an appropriate angle connected just behind the acceleration chamber for introducing the pellet to plasma without destruction. Using the mesh structured components, the horizontal angular distribution of pellets ejected became narrow, because irregular pellet motion caused by sublimated gas was reduced.

To investigate the performance of the injector, pellet injection experiments from the low magnetic field side (LFS) were conducted using ohmic heating plasmas. Central fueling and enhanced fueling rate have been observed. Dα intensity around the divertor region was reduced in a pellet injection plasma compared to gas puffing, indicating low recycling rate was maintained with the pellet injection.

Keywords: JT-60U, Pellet Injector, Centrifugal Acceleration, Deuterium Solid

JT-60Uにおける遠心加速ペレット入射装置の開発

日本原子力研究所那珂研究所核融合装置試験部
木津　要・平塚　一・市毛　尚志・岩橋　孝明・笹島 唯之
正木　圭・佐々木　昇・本田　正男・宮　直之・細金　延幸

(2001年 2月 8日 受理)

JT-60Uプラズマ中心への燃料供給のために重水素固体ペレット入射装置を開発した。本装置は直線型のロッドを回転させ遠心力によってペレットを加速する機構となっており、0.3~1.0 km/sの速度で最大40個(1~10 Hz)で射出可能である。0.7 km/s以下の速度でのペレット1個あたりの平均的な原子数は3.6×10^{20}個である。

加速中にペレットからの昇華ガスにより、ペレットの運動が乱されるのを防ぐために加速部品にメッシュ構造を取り入れ、また射出されたペレットを破壊せずにプラズマまで導くために適切な角度を持ったファンネル（テーパー管）を開発したことにより、破壊なく高い確率でのペレット入射が可能となった。

オーム加熱(OH)プラズマへの低磁場側からのペレット入射実験を行ったところ、ガスパフに比べて中心領域に供給が行えること、ダイバーター領域のDα発光強度も小さく押さえられ低リサイクリングを維持していることを確認した。

那珂研究所：〒311-0193 茨城県那珂郡那珂町向山 801-1

Contents

目次

This is a blank page.

1. Introduction

Considering a future fusion experimental reactor like ITER (International Thermonuclear Experimental Reactor) or a demo reactor like SSTR (Steady State Tokamak Reactor), high density and high confinement plasmas are required of long pulse D-T operations. For attaining such plasmas, refueling of burning particles (D, T) to the core plasma becomes very important. Several techniques such as pellet injection and compact toroid (CT) injection [1] are considered as the refueling technique. Though, gas puffing is the most frequently used method, degradation in plasma confinement has been reported with increasing the electron density in several tokamaks such as JT-60U [2], JET [3] and ASDEX-U [4]. In comparison with the gas puffing, the CT and pellet injections are expected to penetrate deeply inside the plasma, so that the core fueling without degradation of plasma confinement and high fueling efficiency are expected. At present, pellet injection is considered as the realistic fueling method, because CT is still in a stage of development of basic technologies on JFT-2M [5].

There are two types of pellet acceleration system. One is a pneumatic and the other is a centrifugal. In general, pneumatic injector can accelerate the pellet with a high speed of about 2.5 km/s [6], but repetition frequency is still low even though a 10 Hz injector was developed in Oak Ridge National Laboratory (ORNL) [7]. JT-60U also had a pneumatic type pellet injector with 4 barrels (two small and two large pellets) [8] from 1988 to 1996. This injector had an ability of the pellet velocity up to 1.6 km/s. Four pellets could be injected independently with time intervals from 0 to 200 ms. Pellet size was cylindrical shape with 3 mmϕ × 3 mmL or 4 mm ϕ × 4 mmL. On the other hand, a centrifugal pellet injection system has potential for high repetition frequency, like an ASDEX-U injector [9] with 80 Hz. This means that the plasma density can be controlled easily by the feed back control of pellet injection [10]. In JT-60U, development of the centrifugal pellet injector started. The system of centrifugal pellet injector for JT-60U was developed based on the design concept of the ASDEX-U injector [11] which has a straight arm to accelerate the pellet centrifugally and a stop cylinder mechanism to eject the pellet to determined direction.

Pellet injection experiments on several tokamaks have obtained the results of high density plasma with good confinement exceeding the Greenwald density limit [12]. However, decreasing of particle fueling efficiency when pellets were injected from the outside of the torus (low magnetic field side: LFS) was observed as increasing the heating power of NBI [9]. On the other hand, pellet injection from inside of the torus (high magnetic field side: HFS) showed the relatively high fueling efficiency even when NBI is injected [13]. Such a validity of HFS injection has also been observed in DIII-D [14]. Now, tokamaks like ASDEX-U, DIII-D and JET [15] has the system for HFS injection. In this context, a guide tube for HFS injection was also adopted in JT-60U.

In this report, the mechanism of JT-60U pellet injection system, key techniques for developments and test stand results are described. The first results of the pellet injection experiments using the ohmic heating plasmas are also reported. The system of guide tube for HFS injection will be reported elsewhere.

2. System of pellet injector

2.1 Overview of the system

Figure 1 shows the overview of the pellet injector for a test stand. The centrifugal injector consists of three vacuum chambers, referred as "Production chamber", "Acceleration chamber", and "Diagnostic chamber". Figure 2 shows the schematic drawing of production chamber and acceleration chamber. The production chamber has a deuterium supply line, a liquid helium (LHe) lines, a liquefier, a freezer, a piston, a J-tube and cutter. The acceleration chamber includes an acceleration rod. Deuterium pellets produced through the production chamber are accelerated in the acceleration chamber. The process for pellet injection is as follows.

(i) Deuterium supplied from the liquefier is frozen as cylindrical-shape at 12K in the freezer.

(ii) The temperature of freezer is raised up to 15 K. Then, the solid deuterium is pushed by the piston rod and is extruded through the J-tube with square (2.1 mm × 2.1 mm) inner cross section.

(iii) The extruded solid deuterium is cut to cubic (2.1 mm × 2.1 mm × 2.1 mm) pellets which fall into the center of the acceleration rod.

(iv) Pellets are accelerated centrifugally by the straight acceleration rod.

(v) Pellets are injected into the funnel with a wide entrance (65.5 mm). The funnel is connected to the tube to guide pellets to the plasma.

(vi) In a case of testing, pellets which pass through the funnel and microwave cavity in diagnostic chamber for pellet mass measurement are injected into the test chamber to measure the injection efficiency, pellet mass and so on.

2.2 Pellet production

The production chamber was pumped out by a turbo molecular pump and a rotary pump for heat insulation. Pressure of the chamber measured by the ionization vacuum gauge was below $1x10^{-5}$ Pa. As shown in Fig. 1, the production chamber was separated from the acceleration chamber to prevent the intrusion of the sublimated gas from deuterium solid in the acceleration chamber. Such gas raises the temperature of the freezer and J-tube and makes the pellet production unstable. All components in the production chamber were covered by the super insulation mat for reducing the heat transfer by thermal radiation. A liquid helium line from the dewer tank (1000 *l*) was divided to two lines. One line passes through the freezer and the liquefier. The other line passes through the cutter and the J-tube. The temperature of the freezer can be cooled to 9 K. To control the temperature of each component, heaters were fixed on the liquefier, upper and lower parts of the freezer and J-tube. These heaters were electronically controlled to attain the appropriate temperature. Each temperature was monitored by chromel-AuFe (0.07%) thermocouples (KpvsAu7Fe).

The liquefier, freezer and J-tube are made of copper. The size of freezer is 5 mm in inner diameter and 116.5 mm in length. The J-tube is a bent tube to guide the extruded deuterium solid to the cutter. The J-tube is arranged between the freezer and the cutter as shown in Fig. 2. The J-tube has the

2.1 mm x 2.1 mm square inner cross section to shape the deuterium solid to square. The piston extrudes the D_2 solid at the speed of 20 mm/s in maximum. The load on the piston is monitored by a strain gauge for preventing the destruction of piston. The cutter system is constructed by a plunger and a solenoid coil. The plunger has two edges with 2.1 mm in width. The maximum cutting frequency is 20 Hz.

A CCD camera was installed to monitor the extruded deuterium solid through the cutter. From measurements of extrusion length and extrusion duration, the volume of the produced deuterium solid was calculated. The cutter is not operated during these measurements. This system is helpful to optimize the temperature of the each component, D_2 supply pressure, the time sequence for producing the deuterium solid and so on. To monitor the cut pellets, laser sensor was also installed between the cutter and the acceleration chamber. This laser has the circular cross section of 3 mm in diameter. From the measurements of shadowed area and time, falling speed of the pellet and size of the pellets were measured.

2.3 Pellet acceleration

The acceleration chamber includes the straight rod which accelerates pellets centrifugally. Figure 3 shows the components of the acceleration rod, outer rotor, inner rotor and stop cylinder. The outer rotor made of $TiAl_6V_4$ shown in Fig. 3(c) radially accelerates pellets. The length of outer rotor is 900 mm. To keep the rotating balance, the outer rotor has the symmetrical shape. A motor used in a turbo molecular pump (440 *l*) was adopted for rotating the outer rotor. This motor can rotate up to 266 Hz which is equivalent to the 1.0 km/s of pellet velocity. The minimum operation frequency is limited to 80 Hz corresponding to 320 m/s because the oil for the motor can not be circulated below 80 Hz. The vibration sensor was installed to monitor the vibration of rotor. The acceleration rod has the several resonance frequencies of 83, 120, 150, 224 Hz within the operation frequency from 80 to 266 Hz.. The operation around these resonance frequencies could be avoided.

The inner rotor, made of SUS316L (Fig. 3(b)) is fixed on the center of the outer rotor by screws as shown in Fig. 4(a). The pellets fall into the center hall and are guided to the wall of the stop cylinder along the hall. The inner rotor has a roof to prevent pellets from jumping on the inner rotor.

The starting point of pellet acceleration has to be constant for attaining the constant pellet ejection direction. Therefore a stop cylinder was hanged to prevent the transportation of pellet from the inner rotor to the outer rotor (see Fig. 4(b), 4(c)). The stop cylinder made of SUS316L has an open window of 50°. The stop cylinder is fixed to the static support with a small gap between the inner and outer rotor. Pellets are rotated along the inner wall of the stop cylinder, and are transported to the outer rotor through the open window. The starting point of acceleration is fixed by the open window. Since the inner radius of stop cylinder is about 20 mm, actual acceleration length is about 430 mm that equivalents to the 218 degree acceleration rotating angle by simple equation of motion without a friction. The angle of the stop cylinder is easily varied at the outside of the vacuum chamber to adjust the ejection direction.

Figure 4 shows many holes on the stop cylinder wall. The exit side of inner rotor has the slits. Sublimated gas from pellet makes the pellet motion irregular. This kind of effect was often observed

when the stop cylinder without holes was used. For these holes and slits, sublimated gas from pellet was easily removed.

2.4 Pellet transport and diagnostics

Pellets from outer rotor are injected into a funnel (1st and 2nd), and passes through the microwave cavity, flight pipe (3rd funnel) and high speed shutter, and finally arrive to the test chamber. When the injector is installed to the JT-60U vacuum vessel, a separator which can change the LFS or HFS injection is connected to the high speed shutter instead of test chamber as shown in Fig. 13. All funnels and microwave cavity are installed inside the large vacuum tube or vessel for differential pumping as shown in Fig. 1. The differential pumping is important for avoiding the loss of pellet mass. The residual gas heats the pellets and reduces the speed of pellets. To pump out residual gas, all tubes were separated each other. The experimental results of Büchl and Sandmann [16] have shown the divergence angle of the pellet exiting from the tube was about 2°. Therefore, all the gaps between the tubes were determined to satisfy this value to avoid the loss of pellets. The gaps for shutter and gate valve section are determined in the same way.

Another cause for loss of pellet mass is impacting of pellet on the wall over the speed of destruction. As mentioned above, pellets ejected from the acceleration rod enter into the funnel. The schematic view of first and second funnel which total length is 1398 mm is shown in Fig. 5. The funnel is separated to two parts for pumping. If the pellet velocity perpendicular to funnel wall is higher than destruction velocity, the pellet will be broken. Therefore, the angle of the funnel has to be as gentle as possible. The cross section of the funnel guide tube is 65.5 mm in width and 12.6 mm in height at the entrance and 10.6 mm in width and 10.6 mm in height at the exit side. The funnel angle is ±1.2°. From the configuration of funnel and acceleration rod, maximum impact angle of pellet to funnel wall is estimated as 3.4°.

The test chamber connected behind the high speed shutter has the volume of 15 *l*. Pressure increase by pellets was measured by a capacitance manometer. The high speed shutter was used for the measurement of pellet mass. This shutter can shuts within several hundreds ms. For measuring the pellet mass, only one pellet was introduced into the test chamber. The pellet mass was estimated by pressure increase. This technique was also used for the calibration of microwave cavity. The cavity was used for measuring the number and mass of passing pellets. This cavity has a resonant frequency of 5.9890 GHz under TM_{010}. For pellet measurements, the operating frequency was set at 5.9879 GHz. An acoustic emission (AE) sensor was attached to the wall of pellet impact side for detecting the sound of pellet impact. This sensor was also attached to the acceleration chamber wall. Using these acoustic sensors, arrival points of pellets were easily detected.

At present, since no sensor was available for measurements of pellet velocity, the pellets velocity mentioned in this paper was calculated from the equation of motion without any friction. From the equation of motion, pellet velocity is written as

$$vp(\mathrm{m/s}) = 0.64 \times 2\pi f(\mathrm{Hz}) \ , \qquad (1)$$

where f shows the rotational frequency of outer rotor.

3. Results and discussion

The production volume of deuterium solid in the freezer was very sensitive to the temperature and deuterium gas flow rate. The freezer has no cap for deuterium gas at the exit. The cross section of the tube is reduced from ϕ5 mm to 2.1 mm × 2.1 mm at the exit. Therefore, expected scenario of growing of deuterium solid is as follows.

(i) Some part of the introduced deuterium liquid and gas is frozen on the freezer wall. However, most of them flow away as gas through out the J-tube and the cutter, and finally evacuate to the acceleration chamber.

(ii) The frozen layer on the wall grows gradually. Then, the cap is made at the J-tube entrance.

(iii) After several minutes, the freezer is occupied by deuterium solid.

If the temperature is too high, the cap is not made and D_2 solid dose not grow. On the other hand, If the temperature is too low, a cap is produced rapidly at the upper part of the freezer. Therefore, the production volume of D_2 becomes small. Finally, the optimized temperature of the freezer became 12 K. The volume of deuterium solid was easily estimated from extruded length monitored by CCD camera. However, deuterium of 12 K was too hard to extrude at an appropriate piston speed for high frequency pellet injection. For the case of ASDEX [11], extrusion and cutting are another process. However, JT-60U injector has to cut pellets during extrusion. Therefore, temperature of the freezer had to be raised up to 15 K. This temperature was determined from allowable load so that the load on the piston may not exceed the 160 kgf.

After above optimization, extruded deuterium solid became 80 % of freezer volume. It means that the produced solid volume was about 1740 mm^3. Only about 550 mm^3 is used as pellet, because most of solid deuterium remains inside the J-tube. Therefore, the usable number of pellets is about 50. We tried to use this waste volume by conducting the next deuterium production. However this attempt failed. This was probably attributed to the J-tube temperature which cannot be cooled at 20 K. The cutter can operate under 20 Hz, but from the limitation of piston load, 10 Hz is maximum for $(2.1\ mm)^3$ cubic at present. Of course, smaller pellets can be eject at 20 Hz.

Figure 6 is the one of the test stand results which shows the time evolution of the signal from (a) the AE sensor on test chamber, (b) the AE sensor on acceleration chamber and (c) the pressure of test chamber. Pellets were ejected at 5 Hz, V_p = 420 m/s. The signals of Fig. 6(a) shows the arrival of pellets at the test chamber. Figure 6(b) shows the two types of signal. Small signals show the sound of cutter and large ones show the pellet impact on the acceleration chamber wall, indicating the not injected into the funnel. One can clearly see that the AE sensor is the powerful method to follow the arriving and loosing points of pellets. And also the AE sensor can be used for the measurements of time of acceleration and flight. This result shows that all pellets were successfully eject from the outer rotor through the inner rotor and stop cylinder. The efficiency of injection was also easily calculated. Using these types of experiments, the appropriate stop cylinder angle was found. Figure 7 shows the

dependence of the injection efficiency on stop cylinder angle. The injection efficiencies were calculated from the number of arriving pellets to the test chamber divided by the number of cutting pellets. The angle was measured from an arbitrarily determined standard point. Open and closed circles shows the results of 102 Hz (Vp = 410 m/s) and 172 Hz (Vp = 692 m/s), respectively. The pellet speed dependency was not clear. The efficiency was rapidly increased up to about 0.9 between about 184° and 192°. This angle is coincidence with the angle of funnel width, 7.5 degree.

Figure 8 shows the angular distribution of pellets ejected from the outer rotor using the stop cylinder without holes and inner rotor without slits. The angle of exit width of this stop cylinder was 60 °. This measurement was conducted using the aluminum foil attached on the acceleration chamber. After several shots without changing the angle of stop cylinder, the number of holes on aluminum foil caused by pellets impacts were counted versus angle. Comparing with the Fig. 7, angular distribution became very wide. The FWHM is about 26.5 °. This indicates that the gas transparent wall is very effective and that the pellet motion within the stop cylinder become irregular by sublimated gas from pellets. Such effect was also observed in ASDEX injector [11]. Using the laser sensor for falling pellet and AE sensor at test chamber, pellet transportation time from the laser sensor to test chamber was measured. The number of pellets arriving to the test chamber as a function of the transportation time is shown in Fig. 9. Figure 9(a) and 9(b) shows that the results of rotational frequency of outer rotor was 102 and 172 Hz, respectively. Closed circles in Fig. 9(b) shows the results of acceleration components without gas removing mechanism like Fig. 8. The interval of peaks was about 10 ms for 102 Hz and 6 ms for 172 Hz. These results indicate that the peaks show the number of rotating times of pellets inside the stop cylinder. One can clearly see that the most of pellets were ejected within the one rotation when the gas transparent acceleration components are used. On the other hand, the result obtained without no gas transparent (closed circles) shows the broad peak centered around 6 or 7 rotation, indicating that the probability of through the open window is 1/6. On the other hand, the ratio of open window was 60°/360°=1/6. Therefore, this result means that the pellet in the stop cylinder randomly bounced on the stop cylinder wall and did not smoothly round along the stop cylinder wall. Then, pellets which accidentally arrived at the open window move to the outer rotor path. These results indicate again that the removing the sublimated gas from pellets was important for centrifugal injector.

Using such a transparent stop cylinder and inner rotor, the injector of JT-60U attained over 80 % of injection efficiency derived from number of buildup divided by number of cutting ($N_{buildup}$ / $N_{cutting}$), from the velocity of 300 to 700 m/s as shown in Fig. 10. For these experiments, the angle of stop cylinder shown in Fig. 7 was set at 190 degree.

The pellet mass measurements were also conducted introducing one pellet to the test chamber. The pellet mass was measured by pressure increase of test chamber. Figure 11 shows the relative pellet mass dependence on the pellet speed. Pellet mass was normalized by ideal mass of $(2.1\ mm)^3$ cubic. Open circles show that the results of present funnel which has the estimated impact angle of pellet with 3.4° in maximum. The calculated pellets mass were 75±5 % of $(2.1\ mm)^3$ cubic, that is equivalent to the $(1.9\ mm)^3$ cubic. Since no pellets photographs was taken, the shape of ejected pellet was not discussed in

this paper. Pellet whose speed exceeding the 600 m/s has relatively small mass, which is probably attributed to the wear through the funnel. On the other hand, nearly constant masses from 300 to 500 indicate that the pellet mass was already decreased to $(1.9\ mm)^3$ cubic before impact on the funnel wall. The cutting and acceleration processes probably cause such constant mass loss. For the comparison, the results obtained with the old funnel which has estimated maximum impact angle of 4.7° were shown as closed circles. Absolute values of relative mass should not be directly compared with present funnel case, because the conditions of pellets were not completely optimized for old case. However, unlike the present funnel pellet mass which shows the nearly same masses below 600 m/s, pellets mass was rapidly decreased with increasing the speed. This indicates that the angle of funnel is important for preventing the destruction of pellet. The perpendicular velocity to the funnel wall seems to be important parameter here. Several experiments were conducted to investigate the destruction of pellets caused by the impact on the wall [16]. The estimation of a limit velocity is also important for the development of guide tube for HFS injection. A new model for estimating the limit velocity was proposed by Artaud and Géraud [18]. They assumed that the deformation of pellet can be modeled as compression of pellet by two plates. For this model, they used the stress-strain diagram of D_2 solid. Using this model, for the case of old funnel, only 600 m/s exceed the first impact breaking limit meaning that the pellet is broken by one collision at the funnel wall. On the other hand, for the present funnel, the first impact breaking limit becomes 800 m/s. Therefore, the difference of two results in Fig. 11 is probably attributed to the angle of funnel.

Figure 12 shows the results of successive injection into the test chamber under 410 m/s (10 Hz), 410 m/s (5 Hz) and 690m/s (5 Hz). It is clearly seen that from 30 to 40 pellets were almost successively injected. This injector can inject 30 ~ 40 pellets successively at a speed of 700 m/s and a frequency of 10 Hz, and a fueling rate of about 3.6×10^{20} D/pellet.

The pellet injector was installed on the JT-60U vacuum vessel. The configuration of pellets injector and JT-60U vacuum vessel was shown in Fig. 13. The injection axis for LFS is the 150 mm upper of mid plane. A separator which can select the injection direction LFS or HFS was installed instead of the test chamber. The separator is a movable funnel (4th funnel) which has the 581 mm in length. The separator was connected to the 5th funnels for LFS or HFS injection through the gate valve shown as V709 in Fig. 13. The 5th funnel for LFS was connected to the gate valve (GV711) of P-10 horizontal port. The 5th funnel for HFS was connected to the guide tube which is connected to the P-9 upper (vertical) port. The details of guide tube were mentioned elsewhere. Helium dewar tank of 2000 *l* instead of 1000 *l* was used for one week experimental operation. The amount of liquid helium consumption is about 16 l/h.

The first pellet injection experiments from LFS were conducted using OH- plasma. The parameters of the plasma were Ip = 1.5 MA and Bt = 3.24 T. The injection frequency was 5 Hz. Pellet speed was 687 m/s. The time evolutions of normal electron density at r /a ~ 0, 0.35, 0.8 and D_α intensity at divertor region were shown in Fig. 14. The line integrated electron densities at r /a ~ 0.35, 0.8 were measured vertically by FIR laser interferometer. The line integrated electron density at r /a ~ 0 was

measured horizontally by a CO_2 laser interferometer. The pellet injection was started from 6.5 s. The 50 % of Greenwald density was attained only by pellet injections. For the comparison, gas puffing experiment using the feed back control system was conducted. As shown in Fig. 14, the plasma was disrupted at 7 s for the case of gas puffing, indicating the fueling rate can be enhanced using the pellet. The intensity of D_α was low for pellet injection indicating the low recycling. Unlike the gas puffing, electron density was higher at the central region. This result indicates that the pellet can fuel at the central region. This is perhaps because the pellet arrived at the center of plasma. Figure 15 shows the pellet speed dependence of injected pellet mass by open circles. The pellet mass was calculated by the increase of electron density times volume of plasma. Large four signals of each pellet speed were shown. For the comparison, values of $(2.1\ mm)^3$ cubic and $(1.9\ mm)^3$ cubic pellet is shown by solid and broken lines, respectively. Experimental values show almost the same values of test stand results of $(1.9\ mm)^3$. Pellets over 800 m/s were somewhat smaller. This attributed to the destruction on the funnel wall as shown in Fig. 11. Unlike the test stand results, the scattering of pellet masses become wide as observed in Fig. 14. The test stand results shown in Fig. 12 were almost same pellets masses for different pellet speed. This reason is not clear yet. But, pellets mass was considered to decrease before arriving at the vacuum vessel, because pellets suffer the several impacts in passing through five funnels. Pellets injection experiments at the test stand suffer from one impact on the 1st funnel. However, pellets arrived at the plasma suffer several impacts exceeds the speed of failure outbreak limit. Therefore, pellets might be necked and broken in passing through the five funnels.

4. Summary

For achievement of high density and high confinement plasma, the centrifugal pellet injector was successfully developed in JT-60U. This centrifugal pellet injector can eject trains of up to 40 cubic pellets at frequencies of 1-10 Hz and speed of 0.3-1.0 km/s. The average pellet mass is 3.6×10^{20} D/pellet below 0.7 km/s.

The production system which includes the freezer, liquefier and cutter was separated from the acceleration system because deuterium gas sublimated from pellets raises the temperature of the production system. From the optimization for deuterium solid production, the temperature of the liquefier and freezer was determined to be 22 K and 12 K, respectively. When the deuterium was extruded, temperature of the freezer rose up to 15 K. This procedure were needed for sufficient piston extrusion speed to make a $(2.1\ mm)^3$ cubic pellet under allowable load. Acceleration motor could rotate up to 266 Hz corresponding to the pellet velocity of 1.0 km/s. The minimum velocity of pellet was 322 m/s (80 Hz), which is limited by the oil circulation in the acceleration motor.

Acceleration components like the inner rotor and stop cylinder need the gas removing mechanism to attain the narrow horizontal ejection angle. This means that the sublimated gas from pellets make the pellet motion irregular. Injection efficiency attained over 80 % for the pellet velocity range of 300 ~ 700 m/s.

The funnel with an appropriate angle connected to just behind the acceleration chamber is

important for pellets to survive. The angle of funnel was decided to ±1.2 ° estimated impact angle of pellet is 3.4 °. Using this funnel pellet mass was kept as 75±5 % of $(2.1\ mm)^3$ pellets up to 600 m/s.

To investigate the total performance of the injector, pellet injection experiments using ohmic heating plasmas were conducted from the low field side (LFS). Central fueling and enhanced fueling rate were observed. The D_α intensity around the divertor region was reduced for the pellet injection case compared to that for gas puffing case, indicating the low recycling was maintained using pellet injection. Pellet masses estimated from the increment in electron densities were corresponding to the test stand results. However, some small pellets were observed which is probably caused by destruction of pellets through the five funnels.

Acknowledgments

We would like to appreciate to Dr. P. T. Lang of Max Planck Institut für Plasmaphysik for his kind suggestions and help with the development and optimization of JT-60U centrifugal pellet injector. In addition, we are grateful to Dr. M. Shimizu and Dr. M. Kuriyama for their continuous support.

References

[1] Perkins L. J., Ho S. K., Hammer J. H., Nucl. Fusion 28, 1365 (1988)

[2] Asakura N., Shimizu K., Shirai H., Koide Y., and Takizuka T.: Plasma Phys. Control. Fusion, 39, 1295 (1997)

[3] JET Team: Nucl. Fusion, Vol. 39, No. 11Y, 1687 (1999)

[4] Suttrop W., Ryter F., Mertens V., Gruber O., Murmann H., Salzmann H., Schweinzer J., and ASDEX Upgrade team: "Proc. 17th Int. Conf. on Fusion Energy 1998", Yokohama (Vienna: IAEA) Vol. 2, 777 (1999)

[5] Ogawa T., Fukumoto N., Nagata M., Ogawa H., Maeno M., Hasegawa K., Shibata T., Uyama T., Miyazawa J., Kasai S., Kawashima H., Miura Y., Sengoku S., Kimura H., and JFT-2M Group: Nucl. Fusion, Vol. 39, No. 11Y, 1911 (1999)

[6] Frattolillo A., Migliori S., Scaramuzzi F., Combs S. K., Baylor L. R., Foust C. R., Gouge M. J., and Milora S. L.: Rev. Sci. Instrum. 67, 1834 (1996)

[7] Combs S. K., Foust C. R. and Milora S. L.: Rev. Sci. Instrum. 66, 2736 (1995)

[8] Kawasaki K., Hiratsuka H., Takatsu H., Shimizu M., Onozuka M., Uchikawa T., Iwamoto S., and Hashiri N.: "Proc. 15th Symposium on Fusion Technology", 724 (Utrecht, 1988)

[9] Lang P. T., Büchl K., Kaufmann M., Lang R. S., Mertensr V., Müller H. W., Neuhauser J., ASDEX Upgrade Team, and NBI Team: IPP-Report IPP 1/304, (1996)

[10] Lang P. T., Neuhauser J., Büchl K., Kaufmann M., Lang R. S., Lorenz A., Mertens V., Müller H. W., Salzmann H., and ASDEX Upgrade Team: IPP-Report IPP 1/314 (1998)

[11] Lang P. T., Andelfinger C., Beck W., Buchelt E., Büchl K., Cierpka P., Kollotzek H., Lang R. S., Prausner G., Söldner F. X., Ulrich M., and Weber G.: IPP-Report IPP 1/274 (1993)

[12] Greenwald M., Terry J. L., Wolfe S. M., Ejima S., Bell M. G., Kaye S. M., Neilson G. H.: Nucl.

Fusion, Vol. 28, No. 12, 2199 (1998)

[13] Lang P. T., Büchl K., Kaufmann M., Lang R. S., Mertens V., Müller H. W., Neuhauser J., ASDEX Upgrade and NI Teams, Phys. Rev. Lett. Vol. 79, No. 8, 1487 (1997)

[14] Combs S. K., Baylor L. R., Foust C. R., Jernigan T. C., Anderson P. M., and Robinson J. I..: "Proc. 18th IEEE/NPSS Symposium on Fusion Engineering", 202 (Albuquerque, 1999)

[15] Watson M. J., Gadeberg M., Jones T. T. C., Lucock R. M. A., Riccardo V., Tait J., Twynam P., Walden A. D., Wijetunge S., and Willis B.: "Proc. 18th IEEE/NPSS Symposium on Fusion Engineering", 326 (Albuquerque, 1999)

[16] Büchl K. and Sandmann W.: "Proc. 12th Symposium on Fusion Technology", 1507 (Jüelich, 1982)

[17] Combs S. K., Baylor L. R., Foust C. R., Gouge M. J., Jernigan T. C., and Milora S. L.: "Proc. 17th IEEE/NPSS Symposium on Fusion Engineering", 1102 (Sandiego, 1997)

[18] Artaud J. F. and Géraud A.: "Proc. 20th Symposium on Fusion Technology", 971 (Marseille, 1998)

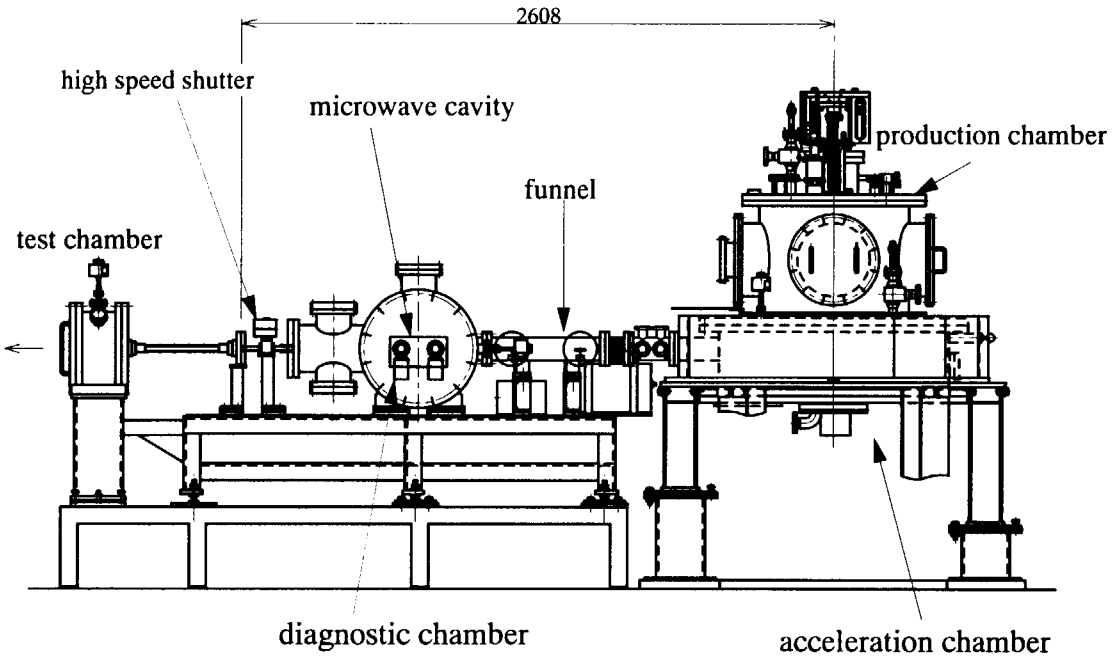

Fig. 1. Overview of the injector for test stand.

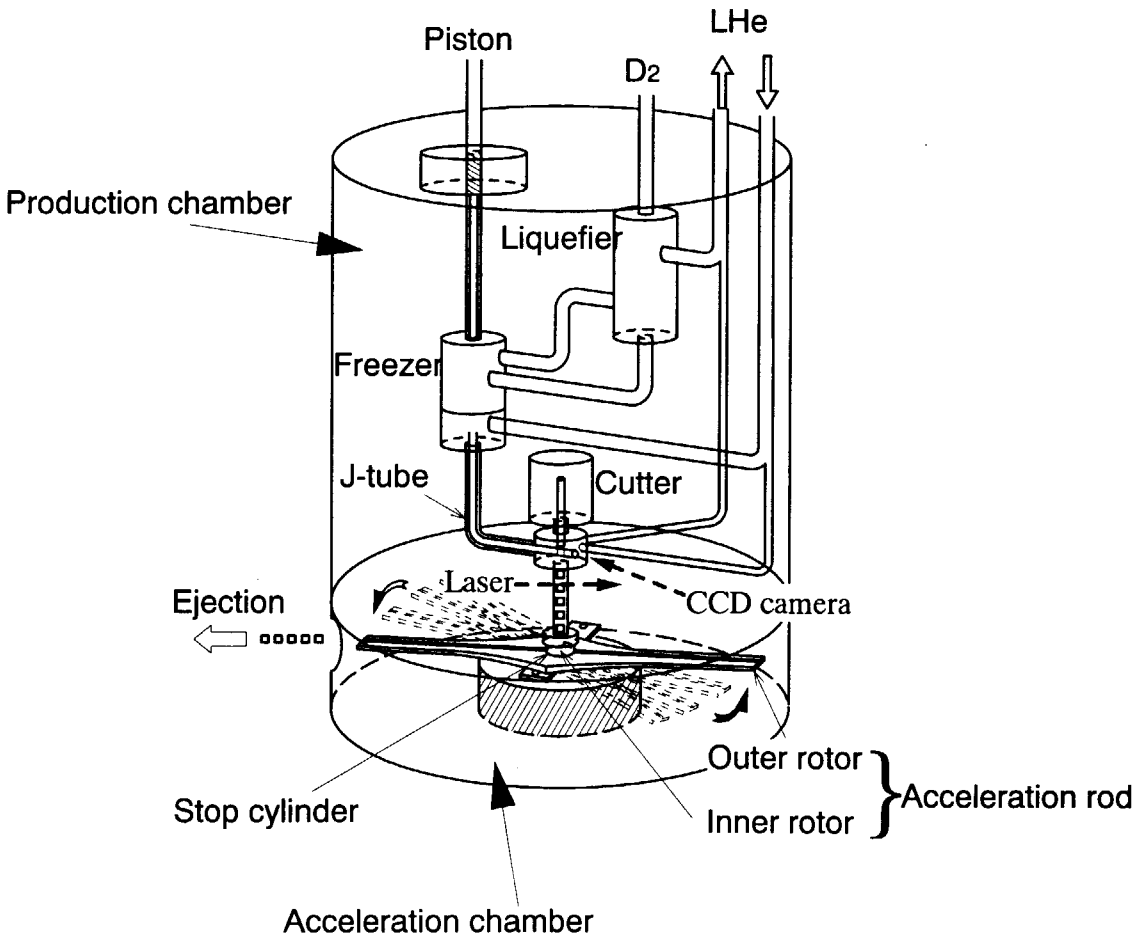

Fig. 2. Schematic drawing of production and acceleration chamber.

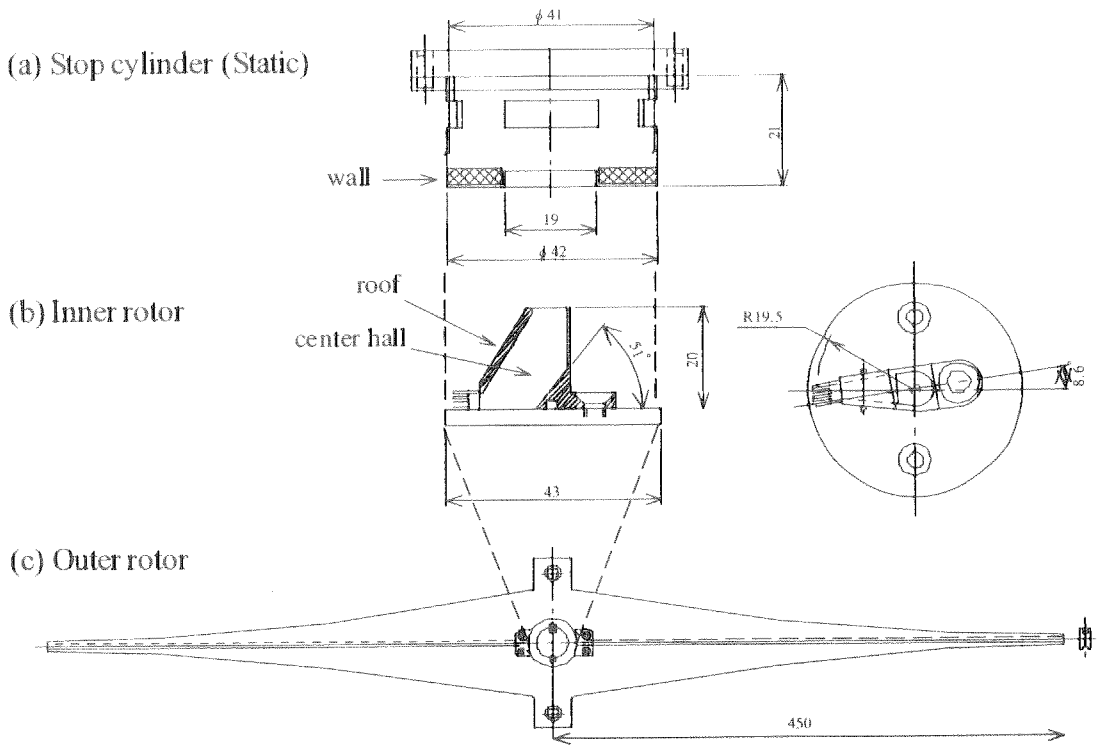

Fig. 3. Components of acceleration rod. (a) The stop cylinder, (b) the inner rotor and (c) the outer rotor.

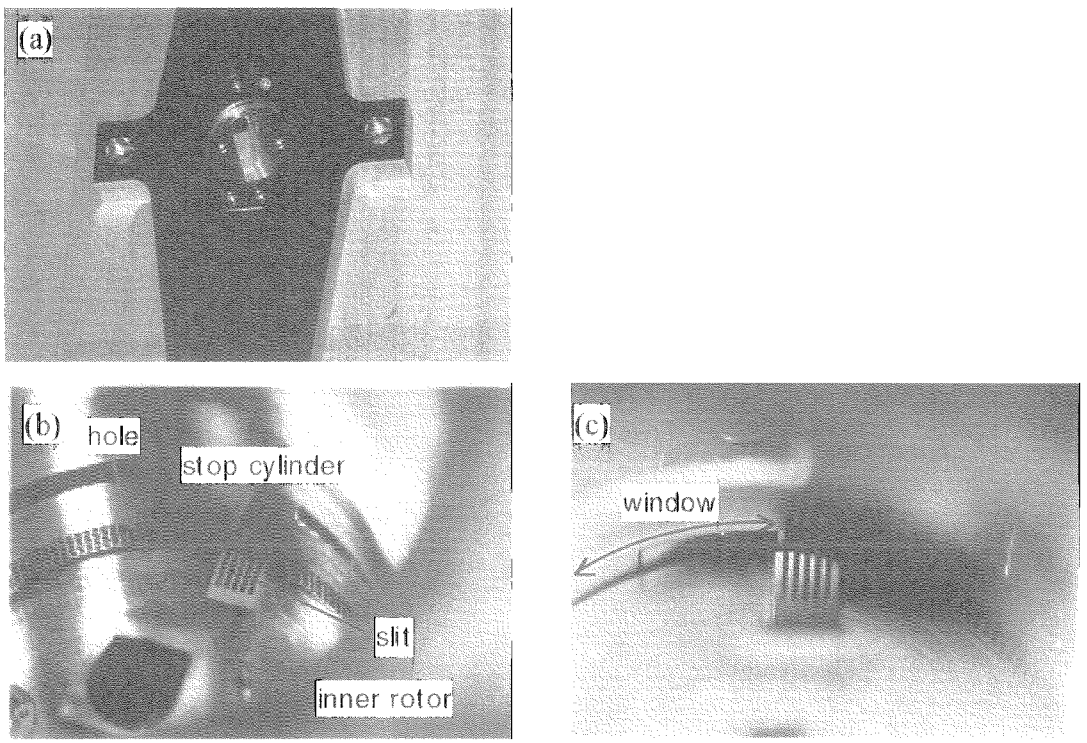

Fig. 4. Photographs of acceleration rod. (a) The inner rotor installed on the outer rotor. (b) The stop cylinder and the inner rotor. (c) The expand view of stop cylinder wall.

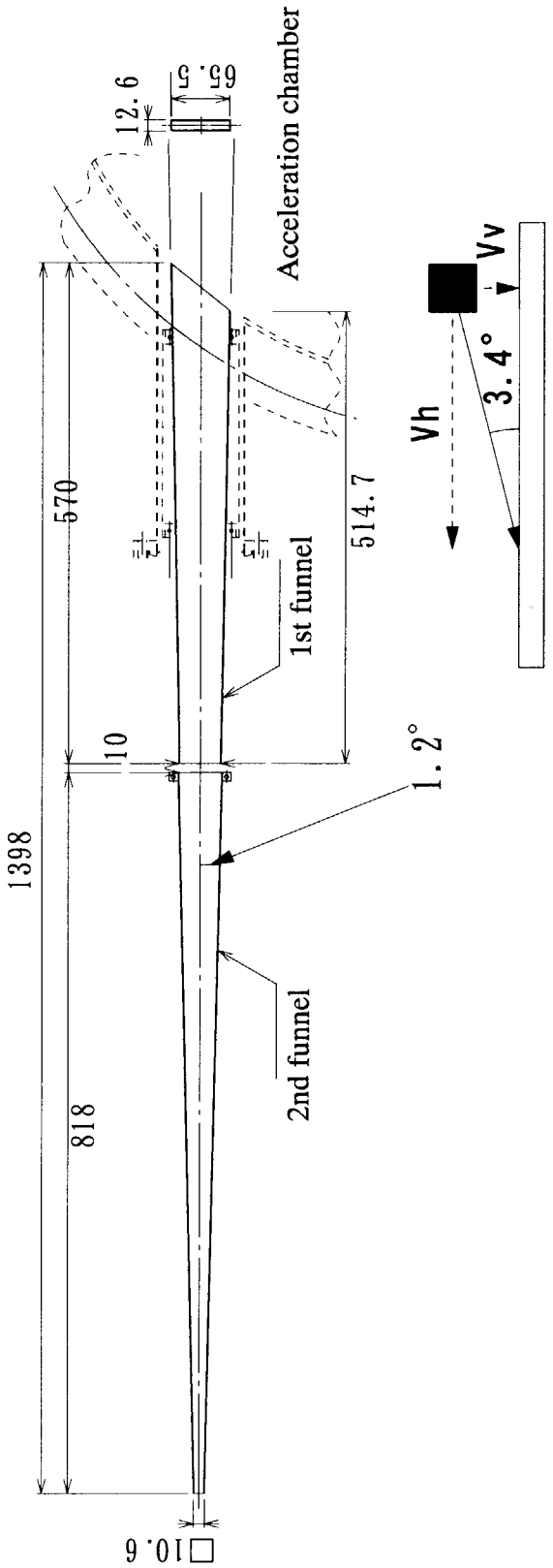

Fig. 5. Schematic drawing of the funnel. The image of pellet impact angle on the wall is also shown.

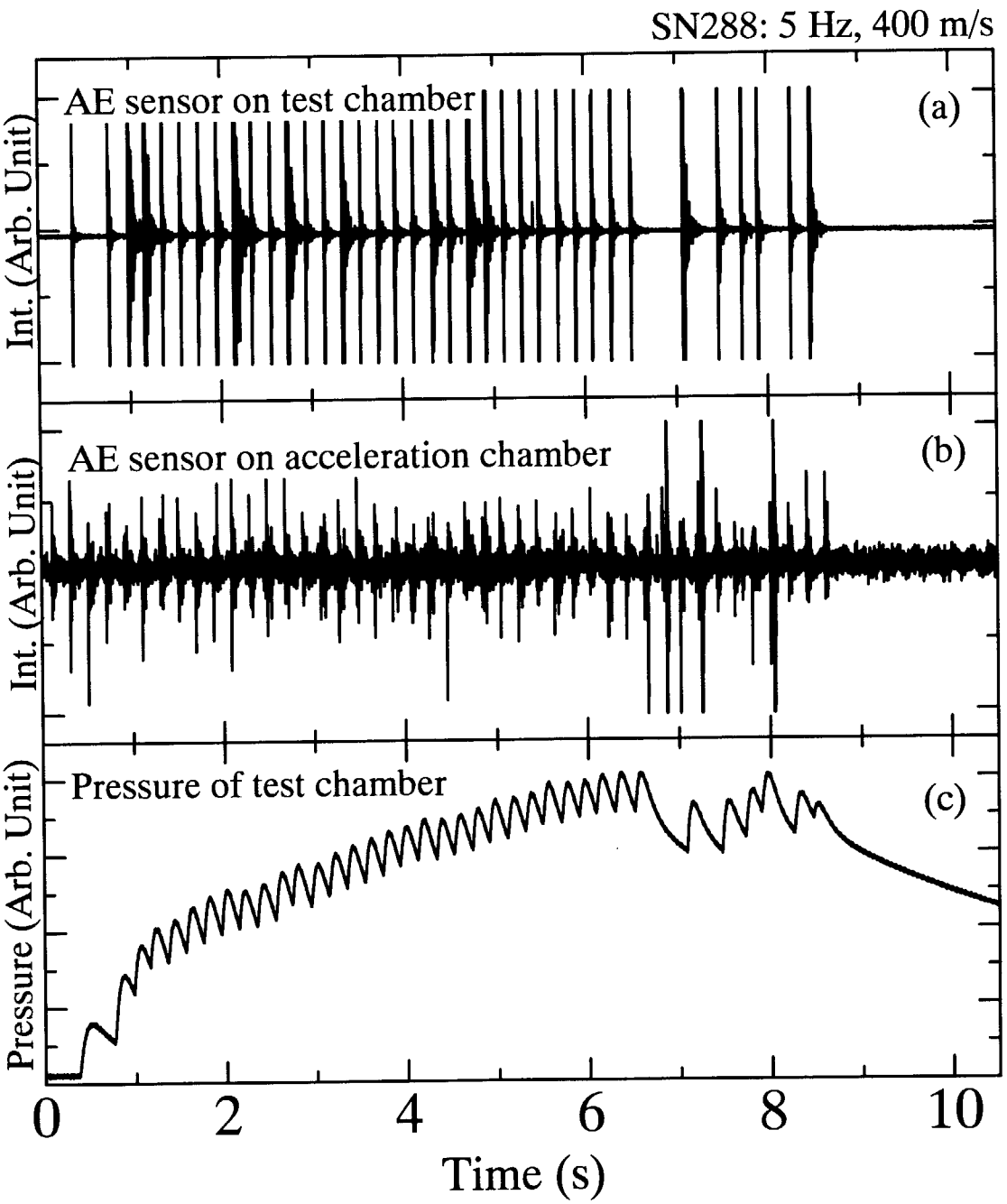

Fig. 6. The one example of test stand results. Time evolution of the signal from (a) the acoustic emission (AE) sensor on test chamber, (b) the AE sensor on acceleration chamber and (c) the pressure of test chamber.

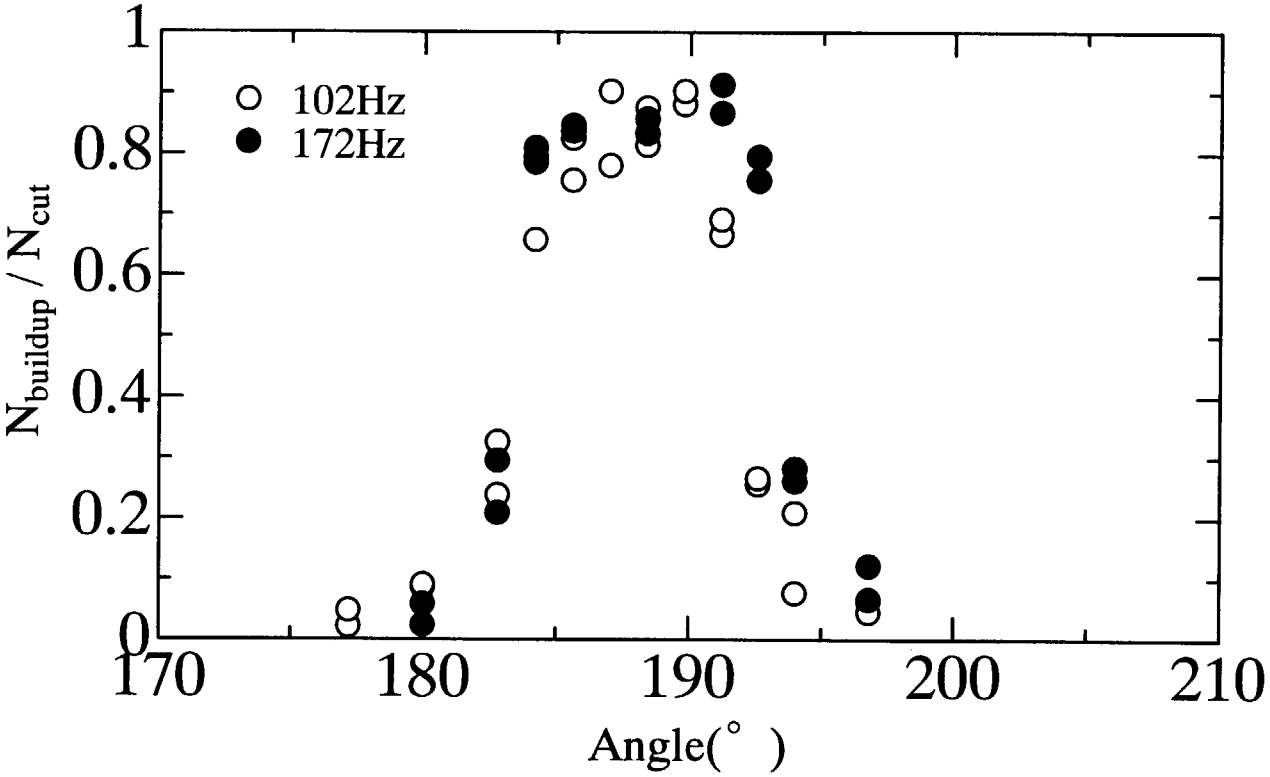

Fig. 7. The stop cylinder angle dependency of injectin efficiency.

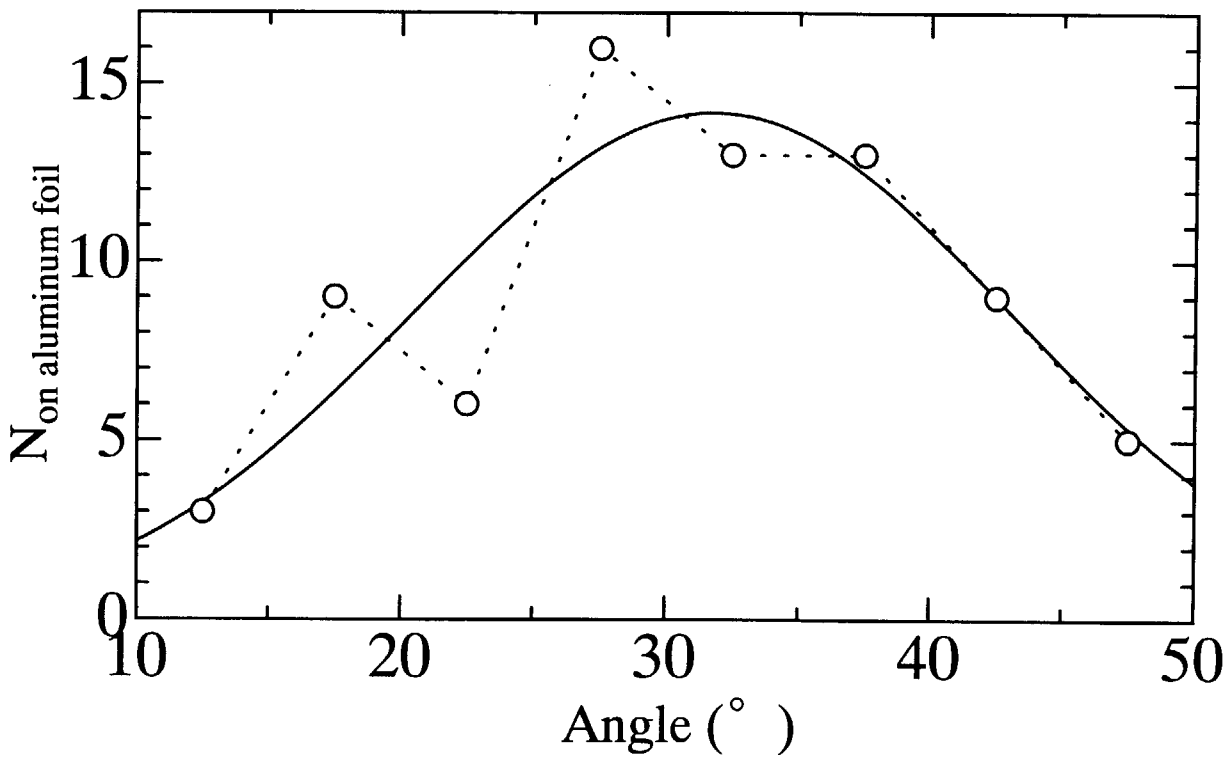

Fig. 8. The horizontal distribution angle of pellet ejection using the no gas transparent stop cylinder and inner rotor.

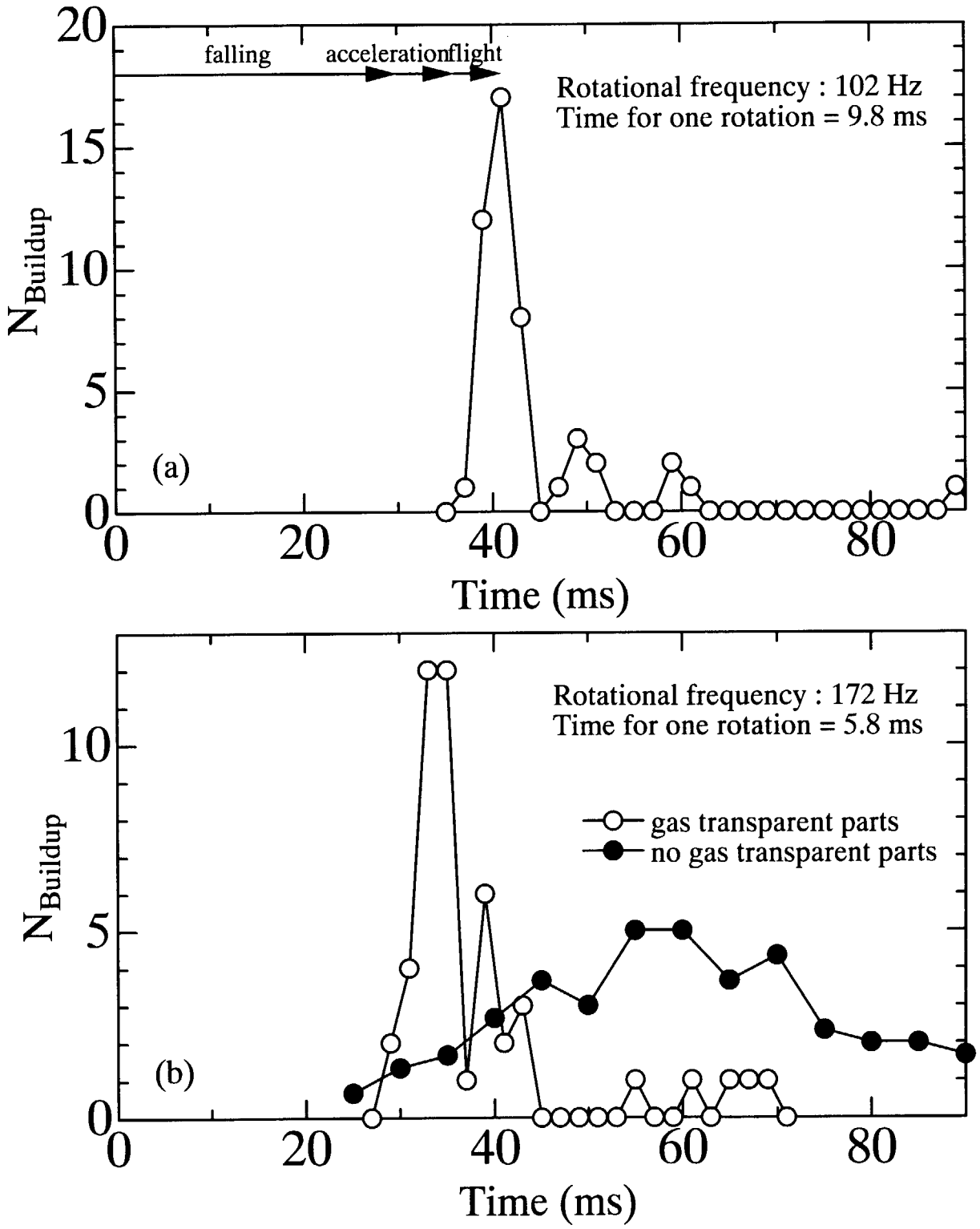

Fig. 9. The time required for pellet transoportaion from laser sensor to test chamber.

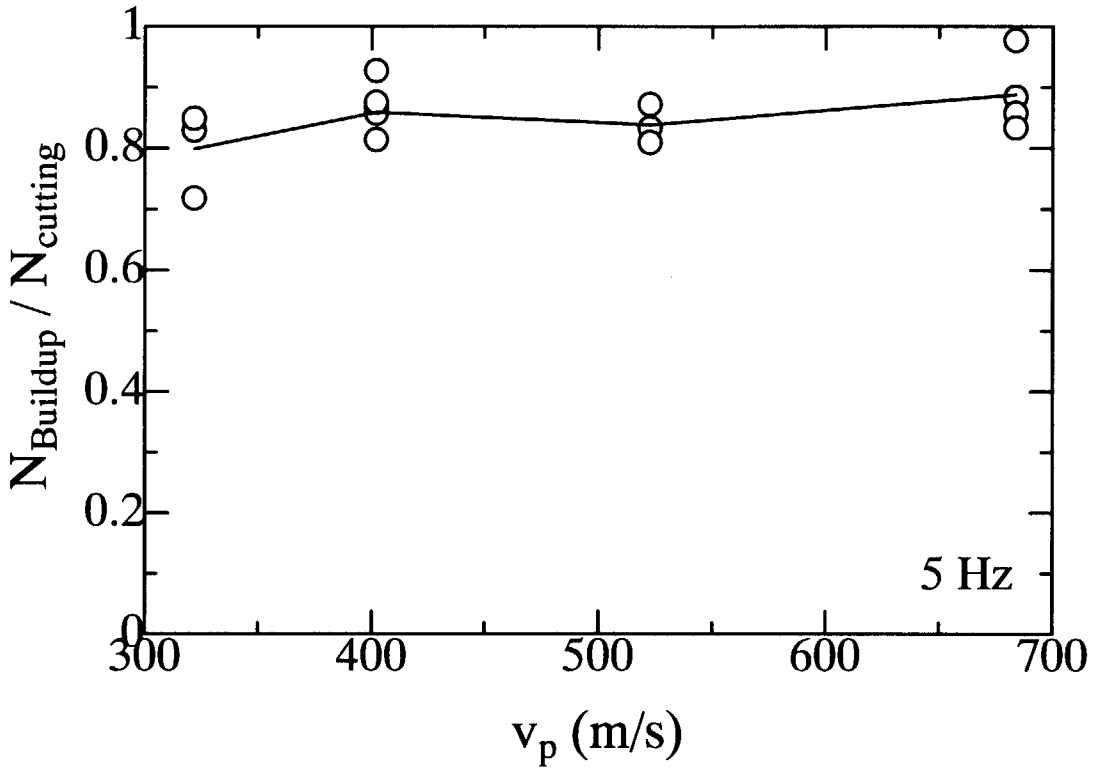

Fig. 10. Pellet velocity dependency of injection efficiency.

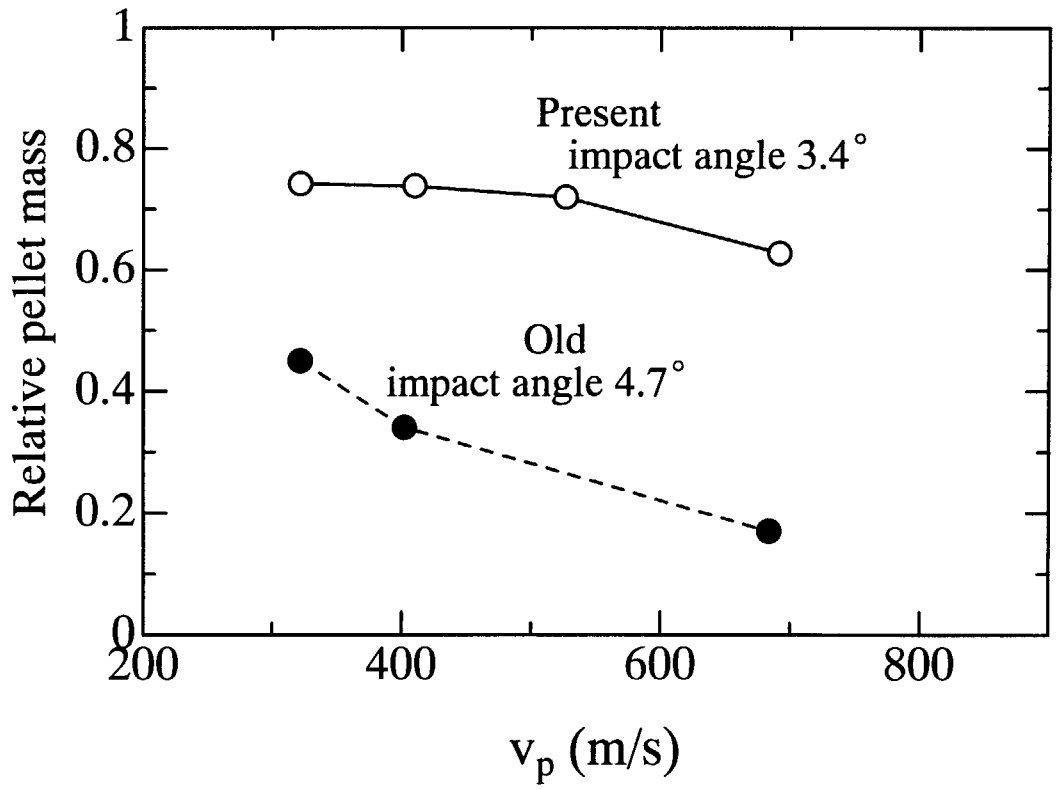

Fig. 11. Pellet velocity dependencies of pellet mass. Pellets masses were normarized by $(2.1\ mm)^3$ cubic.

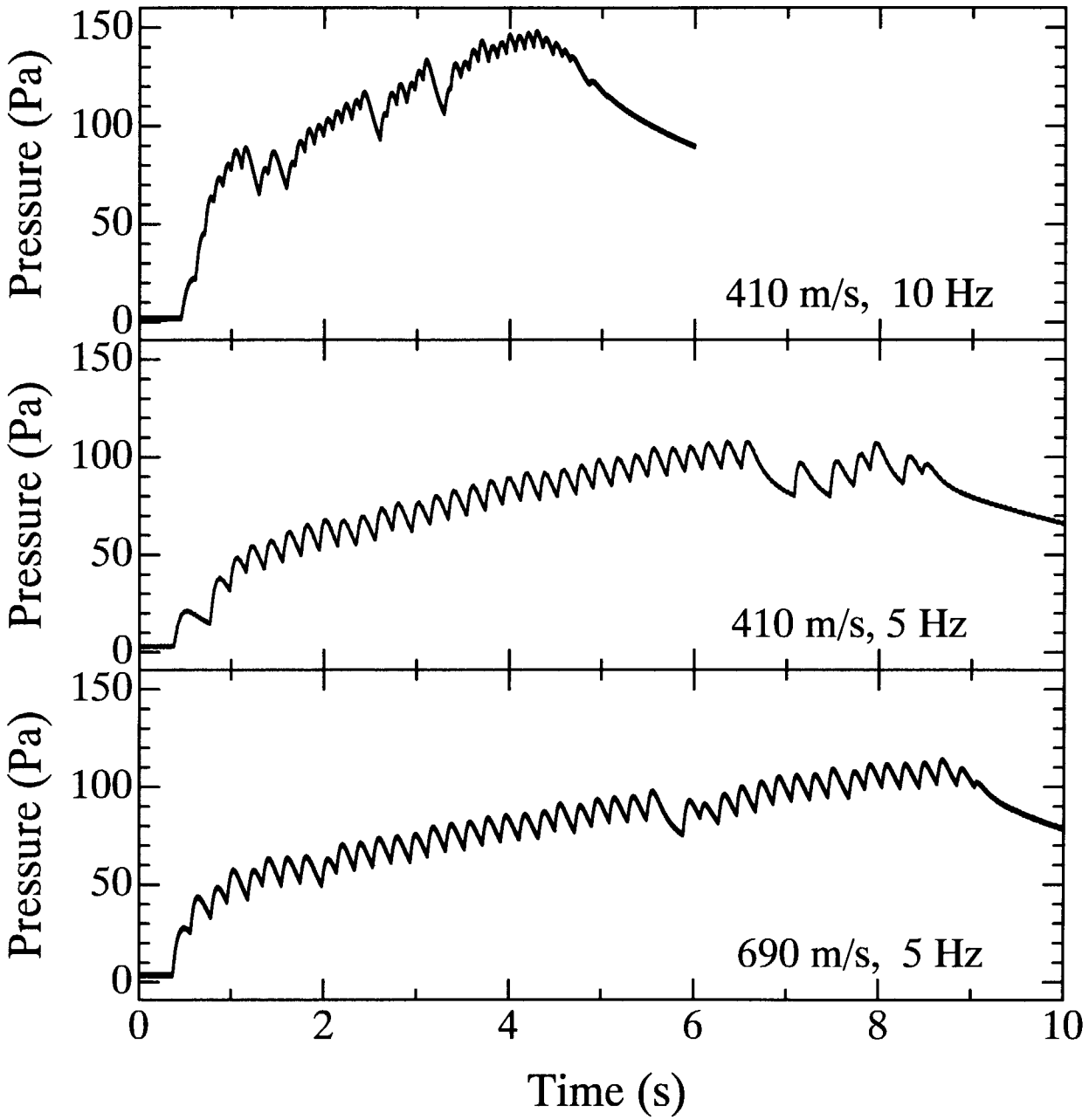

Fig. 12. The results of succesive pellets injection to the test chamber.

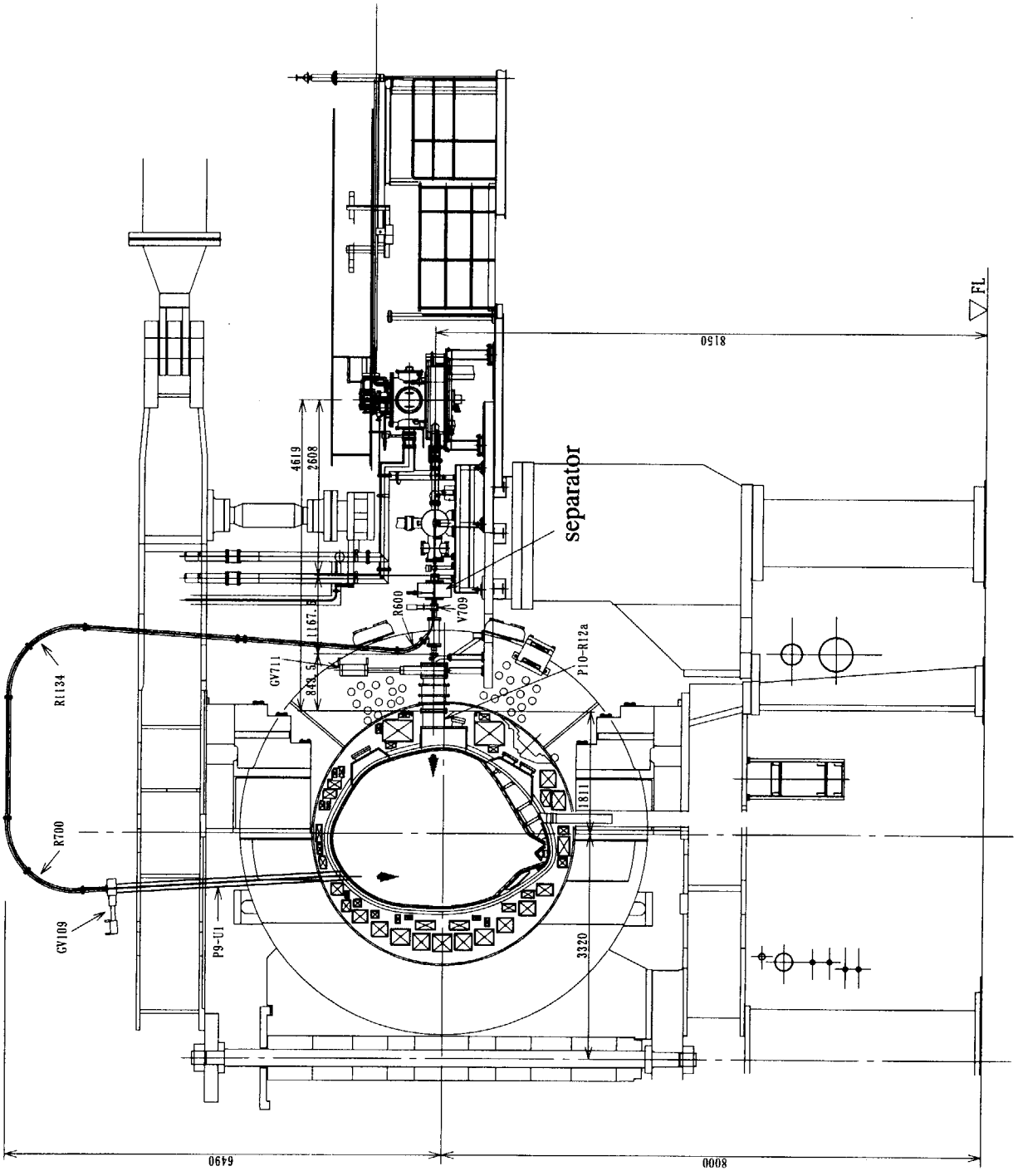

Fig. 13. Installed pellet injector on the JT-60U vacuum vessel.

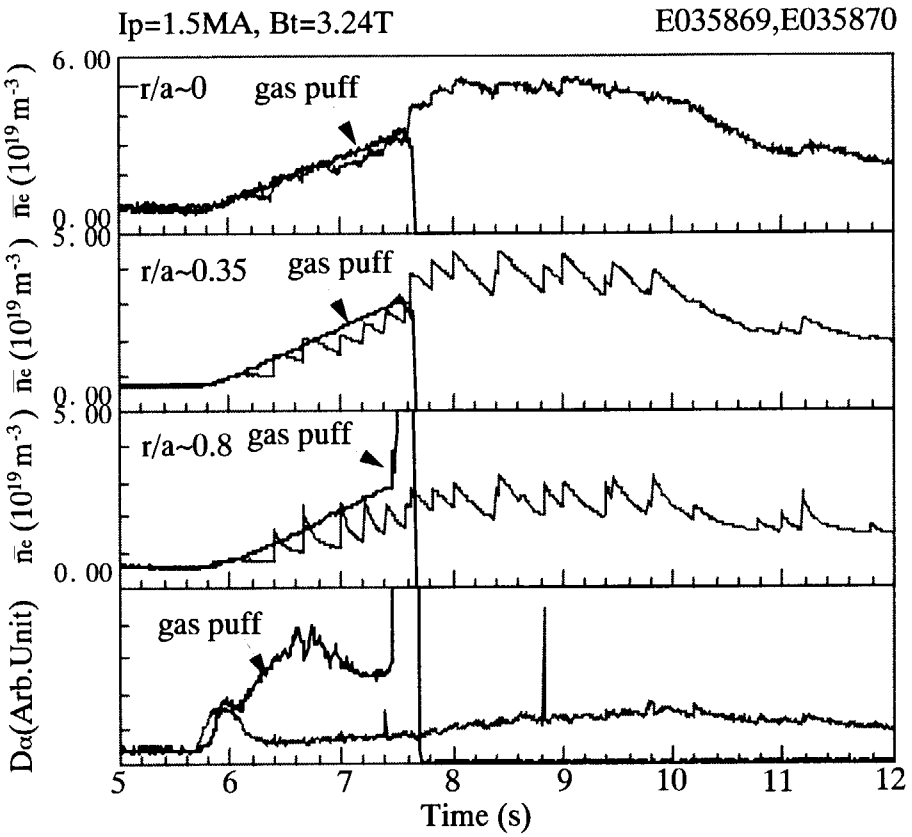

Fig. 14. Time evolution of electron densities and Dα intensity of LFS pellet injection experiment.

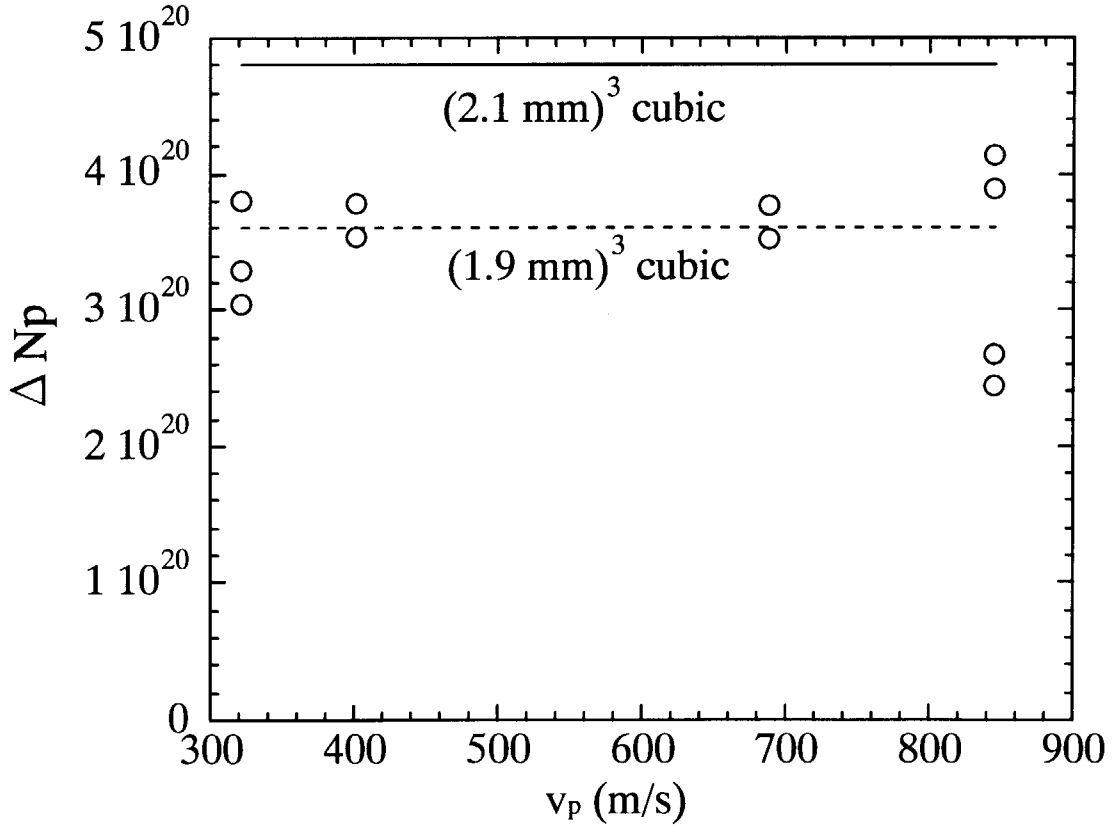

Fig. 15. Velocity dependency of pellet mass estimated from the increase of line density.

国際単位系 (SI) と換算表

表 1　SI基本単位および補助単位

量	名称	記号
長さ	メートル	m
質量	キログラム	kg
時間	秒	s
電流	アンペア	A
熱力学温度	ケルビン	K
物質量	モル	mol
光度	カンデラ	cd
平面角	ラジアン	rad
立体角	ステラジアン	sr

表 2　SIと併用される単位

名称	記号
分，時，日	min，h，d
度，分，秒	°，′，″
リットル	l，L
トン	t
電子ボルト	eV
原子質量単位	u

1 eV = 1.60218 × 10^{-19} J

1 u = 1.66054 × 10^{-27} kg

表 5　SI接頭語

倍数	接頭語	記号
10^{18}	エクサ	E
10^{15}	ペタ	P
10^{12}	テラ	T
10^{9}	ギガ	G
10^{6}	メガ	M
10^{3}	キロ	k
10^{2}	ヘクト	h
10^{1}	デカ	da
10^{-1}	デシ	d
10^{-2}	センチ	c
10^{-3}	ミリ	m
10^{-6}	マイクロ	μ
10^{-9}	ナノ	n
10^{-12}	ピコ	p
10^{-15}	フェムト	f
10^{-18}	アト	a

表 3　固有の名称をもつSI組立単位

量	名称	記号	他のSI単位による表現
周波数	ヘルツ	Hz	s^{-1}
力	ニュートン	N	m·kg/s^2
圧力，応力	パスカル	Pa	N/m^2
エネルギー，仕事，熱量	ジュール	J	N·m
工率，放射束	ワット	W	J/s
電気量，電荷	クーロン	C	A·s
電位，電圧，起電力	ボルト	V	W/A
静電容量	ファラド	F	C/V
電気抵抗	オーム	Ω	V/A
コンダクタンス	ジーメンス	S	A/V
磁束	ウェーバ	Wb	V·s
磁束密度	テスラ	T	Wb/m^2
インダクタンス	ヘンリー	H	Wb/A
セルシウス温度	セルシウス度	℃	
光束	ルーメン	lm	cd·sr
照度	ルクス	lx	lm/m^2
放射能	ベクレル	Bq	s^{-1}
吸収線量	グレイ	Gy	J/kg
線量当量	シーベルト	Sv	J/kg

表 4　SIと共に暫定的に維持される単位

名称	記号
オングストローム	Å
バーン	b
バール	bar
ガル	Gal
キュリー	Ci
レントゲン	R
ラド	rad
レム	rem

1 Å = 0.1 nm = 10^{-10} m

1 b = 100 fm^2 = 10^{-28} m^2

1 bar = 0.1 MPa = 10^5 Pa

1 Gal = 1 cm/s^2 = 10^{-2} m/s^2

1 Ci = 3.7 × 10^{10} Bq

1 R = 2.58 × 10^{-4} C/kg

1 rad = 1 cGy = 10^{-2} Gy

1 rem = 1 cSv = 10^{-2} Sv

（注）

1. 表1－5は「国際単位系」第5版，国際度量衡局 1985年刊行による。ただし，1 eVおよび1 uの値はCODATAの1986年推奨値によった。
2. 表4には海里，ノット，アール，ヘクタールも含まれているが日常の単位なのでここでは省略した。
3. barは，JISでは流体の圧力を表わす場合に限り表2のカテゴリーに分類されている。
4. EC閣僚理事会指令ではbar，barnおよび「血圧の単位」mmHgを表2のカテゴリーに入れている。

換　算　表

力	N(=10^5 dyn)	kgf	lbf
	1	0.101972	0.224809
	9.80665	1	2.20462
	4.44822	0.453592	1

粘度　1 Pa·s(N·s/m^2) = 10 P(ポアズ)(g/(cm·s))

動粘度　1 m^2/s = 10^4 St(ストークス)(cm^2/s)

圧力	MPa(=10 bar)	kgf/cm^2	atm	mmHg(Torr)	lbf/in^2(psi)
	1	10.1972	9.86923	7.50062 × 10^3	145.038
	0.0980665	1	0.967841	735.559	14.2233
	0.101325	1.03323	1	760	14.6959
	1.33322 × 10^{-4}	1.35951 × 10^{-3}	1.31579 × 10^{-3}	1	1.93368 × 10^{-2}
	6.89476 × 10^{-3}	7.03070 × 10^{-2}	6.80460 × 10^{-2}	51.7149	1

エネルギー・仕事・熱量	J(=10^7 erg)	kgf·m	kW·h	cal(計量法)	Btu	ft·lbf	eV
	1	0.101972	2.77778 × 10^{-7}	0.238889	9.47813 × 10^{-4}	0.737562	6.24150 × 10^{18}
	9.80665	1	2.72407 × 10^{-6}	2.34270	9.29487 × 10^{-3}	7.23301	6.12082 × 10^{19}
	3.6 × 10^6	3.67098 × 10^5	1	8.59999 × 10^5	3412.13	2.65522 × 10^6	2.24694 × 10^{25}
	4.18605	0.426858	1.16279 × 10^{-6}	1	3.96759 × 10^{-3}	3.08747	2.61272 × 10^{19}
	1055.06	107.586	2.93072 × 10^{-4}	252.042	1	778.172	6.58515 × 10^{21}
	1.35582	0.138255	3.76616 × 10^{-7}	0.323890	1.28506 × 10^{-3}	1	8.46233 × 10^{18}
	1.60218 × 10^{-19}	1.63377 × 10^{-20}	4.45050 × 10^{-26}	3.82743 × 10^{-20}	1.51857 × 10^{-22}	1.18171 × 10^{-19}	1

1 cal = 4.18605 J (計量法)

= 4.184 J　(熱化学)

= 4.1855 J (15 °C)

= 4.1868 J (国際蒸気表)

仕事率　1 PS (仏馬力)

= 75 kgf·m/s

= 735.499 W

放射能	Bq	Ci
	1	2.70270 × 10^{-11}
	3.7 × 10^{10}	1

吸収線量	Gy	rad
	1	100
	0.01	1

照射線量	C/kg	R
	1	3876
	2.58 × 10^{-4}	1

線量当量	Sv	rem
	1	100
	0.01	1

(86年12月26日現在)